Symmetry Induced Enhancement in Finite-Time Thermodynamic Trade-Off Relations

Ken Funo[*]

Department of Applied Physics, The University of Tokyo, 7-3-1 Hongo, Bunkyo-ku, Tokyo 113-8656, Japan

Hiroyasu Tajima

Graduate School of Informatics and Engineering, The University of Electro-Communications, 1-5-1 Chofugaoka, Chofu, Tokyo 182-8585, Japan

(Received 8 August 2024; revised 22 December 2024; accepted 27 January 2025; published 27 February 2025)

Symmetry imposes constraints on open quantum systems, affecting the dissipative properties in nonequilibrium processes. Superradiance is a typical example in which the decay rate of the system is enhanced via a collective system-bath coupling that respects permutation symmetry. Such a model has also been applied to heat engines. However, a generic framework that addresses the impact of symmetry in finite-time thermodynamics is not well established. Here, we show a symmetry-based framework that describes the fundamental limit of collective enhancement in finite-time thermodynamics. Specifically, we derive a general upper bound on the average jump rate, which quantifies the fundamental speed set by thermodynamic speed limits and trade-off relations. We identify the symmetry condition that achieves the obtained bound, and explicitly construct an open quantum system model that goes beyond the enhancement realized by the conventional superradiance model.

DOI: 10.1103/PhysRevLett.134.080401

Introduction—Symmetry plays a fundamental role in physics, as it provides a powerful tool to analyze, classify, and design the system of interest, and imposes constraints on physical systems such as superselection rules, charge conservations, and so forth. Realistic systems are unavoidably open to their surrounding degrees of freedom, and hence recent studies [1–6] aim to understand the impact of symmetry in open quantum systems. Consequently, discussions based on the symmetry of the Hamiltonian have been extended to those based on non-Hermitian Hamiltonians [7,8] and Gorini-Kossakowski-Sudarshan-Lindblad (GKSL) master equations [9–11]. Symmetry is also related to topology [3–6], degeneracies [12], conserved quantities [2], decoherence-free subspaces, and noiseless subsystems [13], crucial for condensed matter physics and quantum information science.

Symmetry affects not only the equilibrium or steady-state properties of the system, but also the speed and dissipative properties in finite-time and nonequilibrium processes. When we consider permutation-invariant N identical two-level systems, the decay rate can be enhanced by a factor of N via collective system-bath coupling effects, termed superradiance [14,15]. This example implies that symmetry is strongly connected to the notion of collective advantages, which have been extensively studied in the context of quantum thermodynamics, including setups such as heat engines [16–23], quantum batteries [24–26], information erasure protocols [27,28], and photocells [29]. It is therefore expected that designing quantum devices that respect symmetry leads to the suppression of unwanted energetic costs, crucial for charge transport dynamics and quantum information processing protocols. However, a general framework that addresses the influence of symmetry in finite-time and nonequilibrium thermodynamic processes has not been well established.

To develop a general theory to describe the impact of symmetry in finite-time thermodynamics, we pay attention to the thermodynamic speed limit inequalities [30–32] and trade-off relations [20,33], which set generic upper bounds on the speed of state transformation and the change of the expectation values of physical quantities in open quantum systems. These relations indicate that increasing the average jump rate allows having smaller energetic costs (entropy production) while fixing the duration of the process (see Fig. 1). Therefore, investigation of symmetry in thermodynamic trade-off relations provides a unified approach to understanding collective advantages in quantum thermodynamics. Moreover, in view of the close relation between degeneracy and symmetry [12,13], such investigation allows symmetry-based understanding of the effect of degeneracy and coherence on quantum thermodynamics [20].

In this Letter, we develop a generic framework describing the fundamental limit of symmetry-based enhancement in finite-time thermodynamics (see Fig. 1). Specifically, we derive a general upper bound on the average jump rate, showing that the number of degeneracy sets the maximum

[*]Contact author: funo@ap.t.u-tokyo.ac.jp

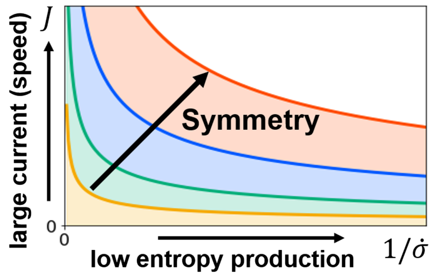

FIG. 1. Schematic picture of the current-dissipation trade-off relation $2J^2/\dot{\sigma} \le A$ [20], where J is the heat current and $\dot{\sigma}$ is the entropy production rate. When the open system dynamics respects certain type of symmetry, the upper bound A can be enhanced (see Fig. 2), and thus higher values of the ratio $J^2/\dot{\sigma}$ can be realized. We derive the fundamental limit of this enhancement [see Eq. (9)].

enhancement. We also derive the symmetry condition on the quantum state and the jump operators that saturates the obtained bound. As an application, we consider a permutation-invariant N two-level systems, and discuss the scaling behavior of the power and efficiency of heat engines, based on the power-efficiency trade-off relation [20]. The obtained theory predicts the possibility of realizing a heat engine that operates near the Carnot efficiency as $\eta = \eta_{\mathrm{Car}} - O(1/N)$, while producing the power that scales from $O(N^2)$ to exponential, which goes beyond the scaling realized by the superradiant heat engine models [17,18].

Setup—We assume that the system of interest is interacting with a heat bath. The interaction Hamiltonian reads $H_{\mathrm{int}} = \sum_a S_a \otimes B_a$, where S_a and B_a are Hermitian operators of the system and the bath, respectively. We describe the reduced dynamics of the system by considering a weak coupling and Born-Markov-secular approximations. Following the standard derivation under these conditions, we obtain the GKSL form of the master equation [9–11] (we take $\hbar = 1$)

$$\partial_t \rho = \mathcal{L}\rho = -i[H, \rho] + \sum_{a,\omega} \gamma_{a,\omega} \mathcal{D}[L_{a,\omega}]\rho, \qquad (1)$$

where $\mathcal{D}[L]\rho = L\rho L^\dagger - (1/2)\{L^\dagger L, \rho\}$ is the dissipator, $\gamma_{a,\omega}$ is the decay rate, and $L_{a,\omega} = \sum_{\omega=\epsilon_k-\epsilon_l} \Pi_l S_a \Pi_k$ is the Lindblad jump operator that let the system jump from one energy eigenstate to another with their energy difference equal to ω. Here, Π_k is the projection to the kth energy eigenspace $\mathcal{S}_k$, and ϵ_k is the kth energy eigenvalue, i.e., $H = \sum_k \epsilon_k \Pi_k$. We denote $\mathcal{N}_k = \dim(\Pi_k)$ as the number of degeneracy of the kth energy. We further assume the detailed balance condition $\gamma_{a,-\omega} = \gamma_{a,\omega} e^{-\beta\omega}$ to make Eq. (1) thermodynamically consistent, where β is the inverse temperature of the heat bath.

One of the main objectives in the field of stochastic thermodynamics is to minimize the entropy production in finite-time processes [34–38]. To this end, we focus on the activity [30,39] $A_{\mathrm{act}} = \sum_\omega A_\omega$ and an activity-like quantity $A = \sum_\omega \omega^2 A_\omega$, where

$$A_\omega(\rho, L_{a,\omega}) = \sum_a \gamma_{a,\omega} \mathrm{Tr}[L_{a,\omega}^\dagger L_{a,\omega} \rho], \qquad (2)$$

is the average jump rate with fixed transition energy ω. Note that these quantities set a timescale of the system and play a fundamental role in stochastic thermodynamics. Specifically, the current-dissipation trade-off relation reads $2J^2/\dot{\sigma} \le A$, where J is the heat current, $\dot{\sigma}$ is the entropy production rate [20,33,40]. This trade-off bound is achievable in specific examples [20]. Therefore, suppressing the entropy production while producing a large heat current becomes possible when the value of A is increased (see Fig. 1).

Moreover, A_ω quantifies the transition rate from a kth energy eigenstate $|\psi_k\rangle$ to a lth energy eigenstate $|\psi_l\rangle$, given by $\sum_{a,\omega} \gamma_{a,\omega} |\langle \psi_l | L_{a,\omega} | \psi_k \rangle|^2 = A_{\epsilon_k - \epsilon_l}(|\psi_k\rangle\langle\psi_k|)$. Therefore, having a large A_ω allows increasing the emission of photons to the environment, with the possibility of realizing the enhancement that goes beyond superradiance.

Symmetry—In what follows, we develop a symmetry-based theory that quantifies the limit of the enhancement of A_ω. To this end, we introduce a symmetry group G and assume that the Hamiltonian H is invariant under this group: $[H, V_g] = 0$ for all $g \in G$, where V_g is a unitary representation of the group. We then classify quantum states and jump operators based on V_g, which constitutes the core of our analysis. We assume in the main text that we take appropriate G and V_g whose precise condition is given in Appendix A, such that the symmetry represented by V_g perfectly characterizes the structure of the energy eigenspaces of H. Note that the examples that we discuss later satisfy this condition. On the other hand, the above condition is not satisfied when G does not represent all the symmetry of the Hamiltonian H, e.g., by choosing G as a trivial group, or by only choosing G as the permutation group for the permutation and even number bit-flip invariant system considered in *example 2*. In Appendix B, we generalize our results to any choice of G and V_g. In particular, the main result (9) is still valid, but the bound is no longer achievable in general; we thus further derive an achievable bound on A_ω.

We point out that $A_\omega(\rho, L_{a,\omega}) = \sum_k p_k A_\omega(\rho_k, L_{a,\omega})$, where $p_k = \mathrm{Tr}[\Pi_k \rho]$, and $\rho_k = \Pi_k \rho \Pi_k / p_k$. This relation motivates us to characterize quantum states ρ by their properties of ρ_k acting on $\mathcal{S}_k$. We now introduce following two special classes of quantum states based on V_g:

(i) *Local states* ρ_k^{loc}, defined by

$$\frac{1}{|G|} \sum_{g \in G} V_g \rho_k^{\mathrm{loc}} V_g^\dagger = \frac{1}{\mathcal{N}_k} \Pi_k. \qquad (3)$$

This definition means that by randomly mixing a local state by unitary operators V_g, it gets completely mixed and becomes the maximally mixed state in $\mathcal{S}_k$. We also introduce the local energy eigenbasis $\mathcal{B}_k^{\rm loc} = \{|\psi_k^{\rm loc}(\alpha)\rangle\}_{\alpha=1}^{\mathcal{N}_k}$ for $\mathcal{S}_k$, where each element of $\mathcal{B}_k^{\rm loc}$ satisfies Eq. (3).

(ii) *Symmetric states* $\rho_k^{\rm sym}$, defined by

$$V_g\rho_k^{\rm sym} = \rho_k^{\rm sym}V_g^\dagger = \rho_k^{\rm sym} \quad \text{for all } g. \tag{4}$$

This definition means that symmetric states do not change by the action of V_g.

Next, we consider the symmetry-based classification of jump operators. To this end, we introduce the following covariant condition (so-called weak symmetry condition) for the Liouvillian $\mathcal{L}(V_g x V_g^\dagger) = V_g\mathcal{L}(x)V_g^\dagger$ for any operator x and for all $g\in G$ [1]. This condition imposes the Liouvillian $\mathcal{L}$ to preserve symmetry. Now, we introduce two special types of the jump operators:

(i) *Local jump operators* $\{L_{a,\omega}^{\rm loc}\}$, defined by

$$\left[(L_{a,\omega}^{\rm loc})^\dagger L_{a,\omega}^{\rm loc}, |\psi_k^{\rm loc}(\alpha)\rangle\langle\psi_k^{\rm loc}(\alpha)|\right] = 0 \quad \text{for all } \alpha. \tag{5}$$

Therefore, local jump operators do not create coherence between local states $|\psi_k^{\rm loc}(\alpha)\rangle$ and $|\psi_k^{\rm loc}(\alpha')\rangle$.

(ii) *Symmetric jump operators* $\{L_{a,\omega}^{\rm sym}\}$, defined by

$$V_g L_{a,\omega}^{\rm sym} = L_{a,\omega}^{\rm sym}V_g^\dagger = L_{a,\omega}^{\rm sym} \quad \text{for all } g. \tag{6}$$

Similar to symmetric states, symmetric jump operator do not change by the action of V_g.

To see why we call $\{L_{a,\omega}^{\rm loc}\}$ and $\{|\psi_k^{\rm loc}(\alpha)\rangle\}$ as local, let us consider a permutation-invariant, N identical two-level systems discussed in *example 1*. We then find that $|\psi_k^{\rm loc}\rangle = |e\rangle^{\otimes k}\otimes|g\rangle^{\otimes N-k}\in\mathcal{B}_k^{\rm loc}$, where $|g\rangle$ and $|e\rangle$ denote the ground and excited states of individual two-level systems. This state $|\psi_k^{\rm loc}\rangle$ is "local" in the sense that it is a tensor product of individual two-level states, and does not have superpositions among different subsystems. We also note that the jump operators $\{\sigma_i^-\}_{i=1}^N$ satisfy Eq. (5), where σ_i^- is the lowering operator that acts "locally" on the ith subsystem. With these in mind, we also call $\rho_k^{\rm loc}$ and $L_{a,\omega}^{\rm loc}$ as local quantum states and local jump operators in generic situations.

In what follows, we utilize the above classification of the quantum states and jump operators and derive general properties of A_ω, including its upper bound.

No enhancement condition—First, we show in the Supplemental Material [41] that

$$A_\omega(\rho^{\rm loc}, \{L_{a,\omega}\}) = \sum_k p_k c_k(L_{a,\omega}), \tag{7}$$

$$A_\omega(\rho, \{L_{a,\omega}^{\rm loc}\}) = \sum_k p_k c_k(L_{a,\omega}^{\rm loc}), \tag{8}$$

TABLE I. Classification of the enhancement of A_ω. If either the state or the jump operator is local, A_ω is given by c_k, and cannot be enhanced [see Eqs. (7) and (8)]. If both the state and the jump operator are symmetric, A_ω is maximally enhanced, characterized by the number of degeneracy $\mathcal{N}_k$ [see Eq. (10)].

	Local jump operator $\{L_{a,\omega}^{\rm loc}\}$	Symmetric jump operator $\{L_{a,\omega}^{\rm sym}\}$
Local state $\rho_k^{\rm loc}$	$c_k(L_{a,\omega}^{\rm loc})$	$c_k(L_{a,\omega}^{\rm sym})$ (no enhancement)
Symmetric state $\rho_k^{\rm sym}$	$c_k(L_{a,\omega}^{\rm loc})$ (no enhancement)	$\mathcal{N}_k c_k(L_{a,\omega}^{\rm sym})$ (maximum enhancement)

where $c_k(L_{a,\omega}) = \mathcal{N}_k^{-1}\sum_a\gamma_{a,\omega}{\rm Tr}[\Pi_k L_{a,\omega}^\dagger L_{a,\omega}\Pi_k]$ is the square of the Hilbert-Schmidt norm of the jump operators acting on the subspace $\mathcal{S}_k$ divided by its dimension, and $\rho^{\rm loc} = \sum_k p_k\rho_k^{\rm loc}$. Note that if we consider a trivial rescaling $\sqrt{\gamma_{a,\omega}}L_{a,\omega}\to\sqrt{C\gamma_{a,\omega}}L_{a,\omega}$, the average jump rate is rescaled as $A_\omega\to CA_\omega$, where C is a constant. Therefore, it would be reasonable to analyze the amount of A_ω in units of some norm of the jump operators, and we have therefore introduced $c_k(L_{a,\omega})$. Equations (7) and (8) show that the norm of the jump operators $c_k(L_{a,\omega})$ sets the value of A_ω if at least one of the state and jump operator is local.

Maximum enhancement condition—We now analyze to what extent A_ω can be enhanced. In the Supplemental Material [41], we show a general upper bound on A_ω, for any density matrix ρ and jump operators $\{L_{a,\omega}\}$, expressed as

$$A_\omega(\rho, \{L_{a,\omega}\}) \le \sum_k p_k\mathcal{N}_k c_k(L_{a,\omega}), \tag{9}$$

showing that A_ω can be enhanced up to $\mathcal{N}_k$ times the norm of jump operators c_k for each kth subspace. The equality condition in (9) is achieved by a combination of symmetric states and jump operators, given by

$$A_\omega(\rho^{\rm sym}, \{L_{a,\omega}^{\rm sym}\}) = \sum_k p_k\mathcal{N}_k c_k(L_{a,\omega}^{\rm sym}), \tag{10}$$

where $\rho^{\rm sym} = \sum_k p_k\rho_k^{\rm sym}$. See Table I for the summary of the scaling of A_ω for different states and jump operators.

In what follows, we show specific examples and construct jump operators that realize better scaling of A_ω compared to the superradiance model. We also show that such jump operators allow enhancing the output power and efficiency of heat engines.

Example 1: Permutation invariance—We now apply our results to a permutation-invariant model. Let the system Hamiltonian be N identical two-level systems $H = (\omega_0/2)\sum_{i=1}^N\sigma_i^z$, where σ_i^z is the z component of the Pauli matrix for the ith system. This Hamiltonian is invariant under interchange of subsystem labels i, and is thus invariant under the permutation group S_N. One example of the local state is given by $|\psi_k^{\mathrm{loc}}\rangle = |e\rangle^{\otimes k} \otimes |g\rangle^{\otimes N-k}$, representing the state with k "local" excitations of the two-level systems. On the other hand, the symmetric state $\rho_k^{\mathrm{sym}} = |\psi_k^{\mathrm{sym}}\rangle\langle\psi_k^{\mathrm{sym}}|$ is given by the symmetric Dicke state $|\psi_k^{\mathrm{sym}}\rangle = \mathcal{N}_k^{-1/2}\sum_g V_g|\psi_k^{\mathrm{loc}}\rangle$, where $\mathcal{N}_k = {}_N C_k$ is the number of degeneracy.

In what follows, we demonstrate the obtained results by explicitly calculating $A_{\omega_0}(\rho_k^{\mathrm{sym}}, L_{a,\omega_0})$ for different jump operators L_{a,ω_0} that removes one excitation from the system. For mixed states $\rho^{\mathrm{sym}} = \sum_k p_k \rho_k^{\mathrm{sym}}$, the scaling of A_ω is simply given by the linear combination $\sum_k p_k A_{\omega_0}(\rho_k^{\mathrm{sym}}, L_{a,\omega_0})$. Note that the case of adding one excitation to the system ($\omega = -\omega_0$) can be similarly obtained by using the jump operators $L_{a,-\omega_0} = L_{a,\omega_0}^\dagger$. In the following, we set $\gamma_{a,\omega_0} = \gamma_\downarrow$.

The symmetric jump operator (6) is given by

$$L_{\omega_0}^{\mathrm{sym}} = \sum_{m=0}^{\lceil N/2 \rceil - 1} L_{\omega_0}^{(m)}, \tag{11}$$

where $L_{\omega_0}^{(m)} = \sum \sigma_{i_1}^- \cdots \sigma_{i_{m+1}}^- \sigma_{l_1}^+ \cdots \sigma_{l_m}^+$ and the summation is taken over $(i_1 < \cdots < i_{m+1}) \neq (l_1 < \cdots < l_m)$, and $\lceil \bullet \rceil$ is the ceiling function. We note that $L_{\omega_0}^{(m)}$ includes all possible combinations of $2m+1$-body jump operators that remove one excitation from the system. Using Eq. (11), we find that $A_{\omega_0}(\rho_k^{\mathrm{sym}}, L_{\omega_0}^{\mathrm{sym}}) = \mathcal{N}_k c_k$, with $c_k = {}_N C_{k-1}\gamma_\downarrow$. When $k = \lceil N/2 \rceil$, we use Stirling's formula and obtain $\mathcal{N}_{N/2} \sim \sqrt{2/(\pi N)}2^N$, showing an exponential scaling (see also Fig. 2).

Note that Eq. (11) consists of many-body system operators, which makes it challenging to realize the above optimal scaling in practice. In the following, we therefore approximate Eq. (11) by taking the first $2n+1$-body terms $L_{\omega_0}^{2n+1\text{-ap}} = \sum_{m=0}^n L_{\omega_0}^{(m)}$ and analyze the scaling of the average jump rate. In particular, the one-body approximation reproduces the collective jump operator $L_{\omega_0}^{1\text{-ap}} = \sum_{i=1}^N \sigma_i^-$, which is used in the study of superradiance [14]. The jump operator $L_{\omega_0}^{1\text{-ap}}$ satisfies strong symmetry [1] $[L_{\omega_0}^{1\text{-ap}}, V_g] = 0$, but does not satisfy Eq. (6). The scaling reads $A_{\omega_0}(\rho_k^{\mathrm{sym}}, L_{\omega_0}^{1\text{-ap}}) = (N-k+1)c_k$ with $c_k = k\gamma_\downarrow$. By considering the next order term $L_{\omega_0}^{3\text{-ap}}$, we find that $A_{\omega_0}(\rho_k^{\mathrm{sym}}, L_{\omega_0}^{3\text{-ap}}) = (N-k+1)[1+(N-k)(k-1)/2]c_k$, with $c_k = k[1+(N-k)(k-1)(k-2)/2]\gamma_\downarrow$. When $k = \lceil N/2 \rceil$, A_{ω_0}/c_k scales $O(N^3)$, compared to the case of $O(N)$ scaling for the conventional superradiance model (see Fig. 2).

Finally, we consider local jump operators $\{\sigma_i^-\}_{i=1}^N$. This set of jump operators satisfies the weak symmetry, but does not satisfy the strong symmetry nor Eq. (6). We find that $A_{\omega_0} = c_k = k\gamma_\downarrow$, consistent with Eq. (8).

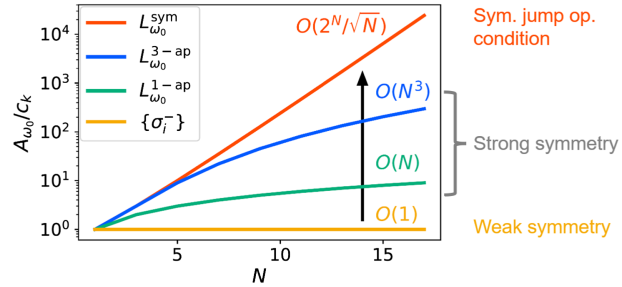

FIG. 2. Plot of $A_{\omega_0}(\rho_k^{\mathrm{sym}}, L_{a,\omega_0})/c_k$ for a permutation-invariant N two-level systems model. We plot the case $k = \lceil N/2 \rceil$, i.e., half of the two-level systems are excited. The red curve is obtained by using the symmetric jump operator $L_{\omega_0}^{\mathrm{sym}}$, demonstrating the optimal enhancement of A_{ω_0}. The blue curve is obtained by using $L_{\omega_0}^{3\text{-ap}}$, showing $O(N^3)$ scaling. The green curve is obtained by using the conventional collective jump operator $L_{\omega_0}^{1\text{-ap}} = \sum_i \sigma_i^-$ in the analysis of superradiance, showing $O(N)$ scaling. The orange line is obtained by using local jump operators $\{\sigma_i^-\}$, demonstrating $A_{\omega_0}/c_k = 1$.

Application of example 1 to heat engines—We apply the permutation-invariant model to the analysis of heat engines. The output power P and the heat-to-work conversion efficiency η of the heat engines satisfy the power-efficiency trade-off relation [20,33]

$$\frac{P}{\eta_{\mathrm{Car}} - \eta} \leq c\bar{A}, \tag{12}$$

where $\eta_{\mathrm{Car}} = 1 - \beta_H/\beta_C$ is the Carnot efficiency; β_H and β_C are the inverse temperatures of the hot and cold baths; $c = \beta_C\eta_{\mathrm{Car}}/[2(2-\eta_{\mathrm{Car}})^2]$ is a constant; and $\bar{A} = \tau^{-1}\int_0^\tau dt \sum_\omega \omega^2 A_\omega$, where τ is the duration of time to complete one engine cycle.

We consider a finite-time quantum Otto heat engine using the jump operators $L_{\pm\omega_0}^{1\text{-ap}}$, $L_{\pm\omega_0}^{3\text{-ap}}$, and $L_{\pm\omega_0}^{\mathrm{sym}}$ (see the Supplemental Material [41] for details). Because of the strong symmetry $[H, V_g] = [L_{a,\omega}, V_g] = 0$, if the initial state is prepared by $\rho^{\mathrm{sym}}(0) = \sum_k p_k(0)\rho_k^{\mathrm{sym}}$, the density matrix at later times remains in the same symmetric Dicke subspace spanned by $|\psi_k^{\mathrm{sym}}\rangle$, and generically takes the form $\rho(t) = \sum_k p_k(t)\rho_k^{\mathrm{sym}}$. Therefore, the scaling of A_ω discussed in the previous section can be directly applied to investigate the scalings of power and efficiency as follows (see also Appendix C).

We choose a protocol such that the efficiency asymptotically reaches the Carnot efficiency as $\eta = \eta_{\mathrm{Car}} - b/N$, where b is a constant [see Fig. 3(a)]. In Fig. 3(b), we show a numerical plot of the output power. The green curve shows the superradiant heat engine setup [17], where the jump operators are given by $L_{\pm\omega_0}^{1\text{-ap}}$. An analytical calculation shows $\bar{A} = O(N)$, and combined with Eq. (12), the power is expected to scale $O(1)$, which is consistent with the

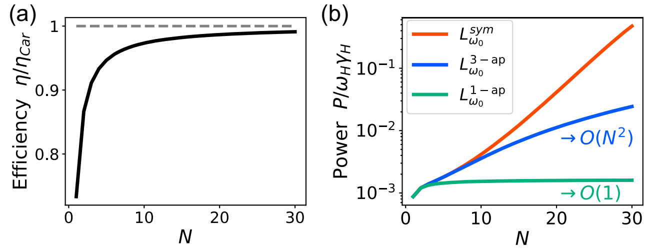

FIG. 3. Plot of the efficiency η/η_{Car} and the power $P/\omega_H\gamma_H$ of the permutation invariant N two-level system heat engine. (a) The efficiency (black curve) scales as $\eta = \eta_{\mathrm{Car}} - b/N$ and asymptotically reaches the Carnot efficiency (gray dashed line). (b) By using the conventional superradiance model ($L^{\text{1-ap}}_{\omega_0}$), the power saturates at large N (green curve). If we use $L^{\text{3-ap}}_{\omega_0}$, the power scales $O(N^2)$ (blue curve), and if we use L_{sym}, the power scales exponentially (red curve). Here, ω_{H} and γ_{H} are the energy level splitting and the decay rate of the system during the hot thermalization stroke, respectively.

numerical plot. If we instead consider $L^{\text{3-ap}}_{\pm\omega_0}$, a similar analysis implies that the power scales $O(N^2)$. By further considering $L^{\mathrm{sym}}_{\pm\omega_0}$, we find an exponential scaling of the power (see Fig. 3).

Example 2: Permutation and even bit flip invariance—We next apply our results to a permutation and even number bit flip (e.g., $V_g = \sigma_i^x\sigma_j^x$) invariant system. The Hamiltonian reads $H = \epsilon\prod_{i=1}^N \sigma_i^z$. When $N = 4$, this Hamiltonian appears in the Kitaev's toric code model as one of the stabilizer operators [49]. The eigenenergies and the number of degeneracies are given by $\pm\epsilon$ and $\mathcal{N}_{\pm\epsilon} = 2^{N-1}$, respectively. The symmetric state reads $|\psi^{\mathrm{sym}}_{\pm\epsilon}\rangle = (|+\rangle^{\otimes N} \pm |-\rangle^{\otimes N})/\sqrt{2}$, where $|\pm\rangle = (|e\rangle \pm |g\rangle)/\sqrt{2}$. The symmetric jump operator reads

$$L^{\mathrm{sym}}_{2\epsilon} = \sum_{m=0}^{\lceil N/2\rceil-1} \sum_{i_1<\cdots<i_{2m+1}} \Pi_{-\epsilon}\sigma^x_{i_1}\cdots\sigma^x_{i_{2m+1}}\Pi_{\epsilon}. \tag{13}$$

Using Eq. (13), we obtain $A_{2\epsilon}(|\psi^{\mathrm{sym}}_\epsilon\rangle\langle\psi^{\mathrm{sym}}_\epsilon|, L^{\mathrm{sym}}_{2\epsilon}) = \mathcal{N}_\epsilon c_\epsilon$ with $c_\epsilon = \mathcal{N}_\epsilon\gamma_\downarrow$, consistent with Eq. (10). This scaling behavior allows us to construct a heat engine model that achieves $\eta_{\mathrm{Car}} - \eta = O(1/\mathcal{N}_\epsilon)$ and $P = O(\mathcal{N}_\epsilon)$ discussed in Ref. [20].

Conclusion—We have shown that the number of degeneracy sets a general upper bound on the average jump rate, and derived a symmetry condition on the quantum states and jump operators that saturates the obtained bound. The obtained results clarify the effect of symmetry in finite-time thermodynamic trade-off relations. As an application, we consider a quantum heat engine composed of permutation invariant N two-level systems. In contrast to the conventional superradiant heat engine model [17,18], we obtained from $O(N^2)$ to exponential enhancement of the output power by designing the jump operators that better respects the obtained symmetry condition.

An interesting future direction is to generalize the obtained framework to generic situations, for example, when the detailed balance is violated [50], the system dynamics is generically non-Markovian [51,52], and there are nonreciprocal interactions [53,54]. The theoretical framework developed in this Letter is anticipated to lead not only to designing high-performance heat engines but also to realizing fast and energy-efficient information processing devices and charge transport devices.

Acknowledgments—We thank Atsushi Noguchi for useful discussions. This work was supported by MEXT KAKENHI Grant-in-Aid for Transformative Research Areas B "Quantum Energy Innovation" Grants No. JP24H00830 and No. JP24H00831. K. F. acknowledges support from JSPS KAKENHI Grant No. JP23K13036 and JST ERATO Grant No. JPMJER2302, Japan. H. T. was supported by JST PRESTO No. JPMJPR2014, JST MOONSHOT No. JPMJMS2061.

[1] B. Buča and T. Prosen, A note on symmetry reductions of the Lindblad equation: Transport in constrained open spin chains, New J. Phys. **14**, 073007 (2012).
[2] V. V. Albert and L. Jiang, Symmetries and conserved quantities in Lindblad master equations, Phys. Rev. A **89**, 022118 (2014).
[3] K. Kawabata, K. Shiozaki, M. Ueda, and M. Sato, Symmetry and topology in non-Hermitian physics, Phys. Rev. X **9**, 041015 (2019).
[4] E. J. Bergholtz, J. C. Budich, and F. K. Kunst, Exceptional topology of non-Hermitian systems, Rev. Mod. Phys. **93**, 015005 (2021).
[5] C.-E. Bardyn, M. A. Baranov, C. V. Kraus, E. Rico, A. İmamoğlu, P. Zoller, and S. Diehl, Topology by dissipation, New J. Phys. **15**, 085001 (2013).
[6] K. Kawabata, A. Kulkarni, J. Li, T. Numasawa, and S. Ryu, Symmetry of open quantum systems: Classification of dissipative quantum chaos, PRX Quantum **4**, 030328 (2023).
[7] R. El-Ganainy, K. G. Makris, M. Khajavikhan, Z. H. Musslimani, S. Rotter, and D. N. Christodoulides, Non-Hermitian physics and PT symmetry, Nat. Phys. **14**, 11 (2018).
[8] C. M. Bender, Making sense of non-Hermitian Hamiltonians, Rep. Prog. Phys. **70**, 947 (2007).
[9] G. Lindblad, On the generators of quantum dynamical semigroups, Commun. Math. Phys. **48**, 119 (1976).
[10] A. K. V. Gorini and E. C. G. Sudarshan, Completely positive dynamical semigroups of N-level systems, J. Math. Phys. (N.Y.) **17**, 821 (2008).
[11] H.-P. Breuer and F. Petruccione, *The Theory of Open Quantum Systems* (Oxford University Press, New York, 2002).

[12] Z. Nussinov and G. Ortiz, A symmetry principle for topological quantum order, Ann. Phys. (Amsterdam) **324**, 977 (2009).

[13] D. A. Lidar, Review of decoherence-free subspaces, noiseless subsystems, and dynamical decoupling, in *Quantum Information and Computation for Chemistry* (John Wiley & Sons, Ltd, New York, 2014), pp. 295–354, 10.1002/9781118742631.ch11.

[14] R. H. Dicke, Coherence in spontaneous radiation processes, Phys. Rev. **93**, 99 (1954).

[15] B. M. Garraway, The Dicke model in quantum optics: Dicke model revisited, Phil. Trans. R. Soc. A **369**, 1137 (2011).

[16] D. Gelbwaser-Klimovsky, W. Niedenzu, P. Brumer, and G. Kurizki, Power enhancement of heat engines via correlated thermalization in a three-level "working fluid", Sci. Rep. **5**, 14413 (2015).

[17] A. Ü. Hardal and Ö. E. Müstecaplıoğlu, Superradiant quantum heat engine, Sci. Rep. **5**, 12953 (2015).

[18] W. Niedenzu and G. Kurizki, Cooperative many-body enhancement of quantum thermal machine power, New J. Phys. **20**, 113038 (2018).

[19] G. Watanabe, B. P. Venkatesh, P. Talkner, M.-J. Hwang, and A. del Campo, Quantum statistical enhancement of the collective performance of multiple bosonic engines, Phys. Rev. Lett. **124**, 210603 (2020).

[20] H. Tajima and K. Funo, Superconducting-like heat current: Effective cancellation of current-dissipation trade-off by quantum coherence, Phys. Rev. Lett. **127**, 190604 (2021).

[21] S. Kamimura, H. Hakoshima, Y. Matsuzaki, K. Yoshida, and Y. Tokura, Quantum-enhanced heat engine based on superabsorption, Phys. Rev. Lett. **128**, 180602 (2022).

[22] B. Yadin, B. Morris, and K. Brandner, Thermodynamics of permutation-invariant quantum many-body systems: A group-theoretical framework, Phys. Rev. Res. **5**, 033018 (2023).

[23] J. Kim, S.-h. Oh, D. Yang, J. Kim, M. Lee, and K. An, A photonic quantum engine driven by superradiance, Nat. Photonics **16**, 707 (2022).

[24] F. C. Binder, S. Vinjanampathy, K. Modi, and J. Goold, Quantacell: Powerful charging of quantum batteries, New J. Phys. **17**, 075015 (2015).

[25] F. Campaioli, F. A. Pollock, F. C. Binder, L. Céleri, J. Goold, S. Vinjanampathy, and K. Modi, Enhancing the charging power of quantum batteries, Phys. Rev. Lett. **118**, 150601 (2017).

[26] J.-Y. Gyhm, D. Šafránek, and D. Rosa, Quantum charging advantage cannot be extensive without global operations, Phys. Rev. Lett. **128**, 140501 (2022).

[27] A. Rolandi, P. Abiuso, and M. Perarnau-Llobet, Collective advantages in finite-time thermodynamics, Phys. Rev. Lett. **131**, 210401 (2023).

[28] Y. Liu, C. Huang, X. Zhang, and D. He, Collective advantages in qubit reset: Effect of coherent qubits, arXiv:2407.03096.

[29] C. Creatore, M. A. Parker, S. Emmott, and A. W. Chin, Efficient biologically inspired photocell enhanced by delocalized quantum states, Phys. Rev. Lett. **111**, 253601 (2013).

[30] K. Funo, N. Shiraishi, and K. Saito, Speed limit for open quantum systems, New J. Phys. **21**, 013006 (2019).

[31] T. Van Vu and K. Saito, Thermodynamic unification of optimal transport: Thermodynamic uncertainty relation, minimum dissipation, and thermodynamic speed limits, Phys. Rev. X **13**, 011013 (2023).

[32] T. Van Vu and Y. Hasegawa, Geometrical bounds of the irreversibility in Markovian systems, Phys. Rev. Lett. **126**, 010601 (2021).

[33] N. Shiraishi and K. Saito, Fundamental relation between entropy production and heat current, J. Stat. Phys. **174**, 433 (2019).

[34] S. Deffner and M. V. S. Bonança, Thermodynamic control—an old paradigm with new applications, Europhys. Lett. **131**, 20001 (2020).

[35] P. Abiuso and M. Perarnau-Llobet, Optimal cycles for low-dissipation heat engines, Phys. Rev. Lett. **124**, 110606 (2020).

[36] M. Esposito, R. Kawai, K. Lindenberg, and C. Van den Broeck, Efficiency at maximum power of low-dissipation carnot engines, Phys. Rev. Lett. **105**, 150603 (2010).

[37] E. Aurell, C. Mejía-Monasterio, and P. Muratore-Ginanneschi, Optimal protocols and optimal transport in stochastic thermodynamics, Phys. Rev. Lett. **106**, 250601 (2011).

[38] R. Kosloff and Y. Rezek, The quantum harmonic otto cycle, Entropy **19**, 136 (2017).

[39] N. Shiraishi, K. Funo, and K. Saito, Speed limit for classical stochastic processes, Phys. Rev. Lett. **121**, 070601 (2018).

[40] N. Shiraishi, K. Saito, and H. Tasaki, Universal trade-off relation between power and efficiency for heat engines, Phys. Rev. Lett. **117**, 190601 (2016).

[41] See Supplemental Material at http://link.aps.org/supplemental/10.1103/PhysRevLett.134.080401, for general properties of A_ω for different states and jump operators, including its upper bound. We also give additional details on the setup, examples, and the heat engine setup shown in the main text, which includes Refs. [42–48].

[42] J. P. Pekola, B. Karimi, G. Thomas, and D. V. Averin, Supremacy of incoherent sudden cycles, Phys. Rev. B **100**, 085405 (2019).

[43] A. M. Eriksson, T. Sépulcre, M. Kervinen, T. Hillmann, M. Kudra, S. Dupouy, Y. Lu, M. Khanahmadi, J. Yang, C. Castillo-Moreno, P. Delsing, and S. Gasparinetti, Universal control of a bosonic mode via drive-activated native cubic interactions, Nat. Commun. **15**, 2512 (2024).

[44] M. Müller, K. Hammerer, Y. L. Zhou, C. F. Roos, and P. Zoller, Simulating open quantum systems: From many-body interactions to stabilizer pumping, New J. Phys. **13**, 085007 (2011).

[45] C. Monroe, W. C. Campbell, L.-M. Duan, Z.-X. Gong, A. V. Gorshkov, P. W. Hess, R. Islam, K. Kim, N. M. Linke, G. Pagano, P. Richerme, C. Senko, and N. Y. Yao, Programmable quantum simulations of spin systems with trapped ions, Rev. Mod. Phys. **93**, 025001 (2021).

[46] O. Katz, M. Cetina, and C. Monroe, n-body interactions between trapped ion qubits via spin-dependent squeezing, Phys. Rev. Lett. **129**, 063603 (2022).

[47] O. Katz, M. Cetina, and C. Monroe, Programmable n-body interactions with trapped ions, PRX Quantum **4**, 030311 (2023).

[48] S. Kamimura, K. Yoshida, Y. Tokura, and Y. Matsuzaki, Universal scaling bounds on a quantum heat current, Phys. Rev. Lett. **131**, 090401 (2023).
[49] A. Kitaev, Fault-tolerant quantum computation by anyons, Ann. Phys. (Amsterdam) **303**, 2 (2003).
[50] R. Alicki, M. Šindelka, and D. Gelbwaser-Klimovsky, Violation of detailed balance in quantum open systems, Phys. Rev. Lett. **131**, 040401 (2023).
[51] H.-P. Breuer, E.-M. Laine, J. Piilo, and B. Vacchini, Colloquium: Non-Markovian dynamics in open quantum systems, Rev. Mod. Phys. **88**, 021002 (2016).
[52] I. de Vega and D. Alonso, Dynamics of non-Markovian open quantum systems, Rev. Mod. Phys. **89**, 015001 (2017).
[53] A. Metelmann and A. A. Clerk, Nonreciprocal photon transmission and amplification via reservoir engineering, Phys. Rev. X **5**, 021025 (2015).
[54] A. A. Clerk, Introduction to quantum non-reciprocal interactions: From non-Hermitian Hamiltonians to quantum master equations and quantum feedforward schemes, SciPost Phys. Lect. Notes 44 (2022).
[55] R. Goodman, N. R. Wallach *et al.*, *Symmetry, Representations, and Invariants* (Springer, New York, 2009), Vol. 255.
[56] P. Etingof, O. Golberg, S. Hensel, T. Liu, A. Schwendner, D. Vaintrob, and E. Yudovina, Introduction to representation theory, arXiv:0901.0827.

End Matter

Appendix A: Details on the choice of G and V_g assumed in the main text—In this Appendix, we show technical details on the appropriate choice of G and V_g assumed in the main text. We again note that the main result (9) can be generalized to arbitrary G and V_g, as shown in Appendix B.

To begin with, we note that the commutation relation $[V_g, H] = 0$ implies $[V_g, \Pi_k] = 0$. Then, V_g can be decomposed as $V_g = \bigoplus_k V_g^k$, where V_g^k acts on $\mathcal{S}_k$. Each V_g^k is further decomposed into irreducible representations as $V_g^k = \bigoplus_j I_{\mathcal{H}_j^k} \otimes \mathcal{V}_j^k(g)$, where $\mathcal{S}_k$ is decomposed as $\mathcal{S}_k = \bigoplus_j \mathcal{H}_j^k \otimes \mathcal{K}_j^k$, $\mathcal{V}_j^k(g)$ is an irreducible representation of G acting on the subspace $\mathcal{K}_j^k$, $I_{\mathcal{H}_j^k}$ is the identity matrix acting on the subspace $\mathcal{H}_j^k$, and j labels irreducible representations [22,55,56]. Here, a representation $\mathcal{V}_j^k(g)$ of G acting on $\mathcal{K}_j^k$ is called irreducible if $\mathcal{K}_j^k$ has no nontrivial subspace that is invariant under the action of $\mathcal{V}_j^k(g)$ for all g. Therefore, the subspace $\mathcal{H}_j^k$ is invariant under the operation of V_g^k, and $\mathcal{K}_j^k$ is the only subspace in which V_g^k nontrivially acts on. When there exist (j, k) such that $\dim(\mathcal{H}_j^k) \geq 2$, the symmetry represented by V_g does not perfectly characterize the structure of the energy eigenspaces of H, due to these invariant subspaces. Fortunately, for a given H, we can always take appropriate G and V_g that satisfies $\dim(\mathcal{H}_j^k) = 1$ for any j and k (see the Supplemental Material [41]). We also note that the examples we discuss in the main text satisfy the condition $\dim(\mathcal{H}_j^k) = 1$ for any j and k for natural G and V_g. Therefore, in the main text, we assume that we take appropriate G and V_g that satisfy $\dim(\mathcal{H}_j^k) = 1$ for any j and k. In Appendix B, we discuss the case $\dim(\mathcal{H}_j^k) \geq 2$ and generalize the main results.

Appendix B: Generalization to arbitrary G and V_g—We now show how the main results are generalized to the case of $\dim(\mathcal{H}_j^k) \geq 2$, i.e., arbitrary G and V_g. To begin with, we introduce operators $\sigma_{j,k}$ and $B_{j,k}^{\omega}$ acting on the subspace $\mathcal{H}_j^k$ to parametrize quantum states and jump operators as

$$[\rho_k]_{\mathrm{inv}} = \frac{1}{\sum_j \mathrm{Tr}[\sigma_{j,k}]} \bigoplus_j \sigma_{j,k} \otimes \frac{I_{\mathcal{K}_j^k}}{\dim(\mathcal{K}_j^k)}, \tag{B1}$$

$$\left[\sum_a \gamma_{a,\omega} L_{a,\omega}^{\dagger} L_{a,\omega}\right]_{\mathrm{inv}} = \bigoplus_{k,j} B_{j,k}^{\omega} \otimes \frac{I_{\mathcal{K}_j^k}}{\dim(\mathcal{K}_j^k)}, \tag{B2}$$

where $[X]_{\mathrm{inv}} \coloneqq |G|^{-1} \sum_{g \in G} V_g X V_g^{\dagger}$. We again note that when $\dim(\mathcal{H}_j^k) \geq 2$, $\mathcal{H}_j^k$ is a nontrivial invariant subspace under the action of V_g, and the specific form of $\sigma_{j,k}$ and $B_{j,k}^{\omega}$ cannot be constrained based on the symmetry conditions for given G and V_g. Nevertheless, a general upper bound on the average jump rate can be derived as (see Supplemental Material [41] for details)

$$\begin{aligned} A_{\omega}(\rho, \{L_{a,\omega}\}) &\leq \sum_k p_k \mathcal{N}_k c_k(L_{a,\omega}) F(\sigma_{j,k}, B_{j,k}^{\omega}) \\ &\leq \sum_k p_k \mathcal{N}_k c_k(L_{a,\omega}), \end{aligned} \tag{B3}$$

where

$$F(\sigma_{j,k}, B_{j,k}^{\omega}) = \frac{\sum_j \mathrm{Tr}[\sigma_{j,k} B_{j,k}^{\omega}]}{\sum_j \mathrm{Tr}[\sigma_{j,k}] \sum_j \mathrm{Tr}[B_{j,k}^{\omega}]} \leq 1, \tag{B4}$$

quantifies the overlap between $\{\sigma_{j,k}\}_j$ and $\{B_{j,k}^{\omega}\}_j$. The obtained relation (B3) generalizes the result Eq. (9) to the case of $\dim(\mathcal{H}_j^k) \geq 2$. It should be noted that the bound (9) remains valid in this general case; however, the last equality condition in (B3) can no longer be characterized by the properties of V_g. On the other hand, the first inequality in (B3) is achievable by using symmetric states and jump operators (see Supplemental Material [41] for details)

$$A_\omega(\rho^{\rm sym},\{L^{\rm sym}_{a,\omega}\}) = \sum_k p_k \mathcal{N}_k c_k(L^{\rm sym}_{a,\omega}) F(\sigma^{\rm sym}_{j,k}, B^{{\rm sym},\omega}_{j,k}). \tag{B5}$$

As shown in Eqs. (10) and (B5), symmetric states and jump operators achieve the upper bound of the enhancement of A_ω. It should be noted that the existence of symmetric states and jump operators requires condition $\dim(\mathcal{K}^k_j) = 1$ for one j, which we denote as $j_{\rm sym}$; note that $\sigma^{\rm sym}_{j,k} = B^{{\rm sym},\omega}_{j,k} = 0$ for $j \neq j_{\rm sym}$ is satisfied for symmetric states and jump operators. This condition $\dim(\mathcal{K}^k_{j_{\rm sym}}) = 1$ is not necessarily satisfied for arbitrary G and V_g. Therefore, this condition $\dim(\mathcal{K}^k_{j_{\rm sym}}) = 1$ can be viewed as a design principle of the Hamiltonian and jump operators to achieve the maximum enhancement of A_ω. Note that the examples that we discuss in the main text satisfy this condition. We also note that when $\dim(\mathcal{H}^k_j) = 1$, $\rho^{\rm sym}_k$ is unique (if it exists) and can be written as $\rho^{\rm sym}_k = |\psi^{\rm sym}_k\rangle\langle\psi^{\rm sym}_k|$, where $|\psi^{\rm sym}_k\rangle$ is defined by $V_g|\psi^{\rm sym}_k\rangle = |\psi^{\rm sym}_k\rangle$ for all g.

Appendix C: Scaling of A—Because the density matrix during a heat engine cycle is generically given by a mixed state, here we consider the model discussed in example 1 and show an additional plot that demonstrates the scaling of A for $\rho^{\rm sym}_{\rm th} = \sum_k p^{\rm th}_k \rho^{\rm sym}_k$, where $p^{\rm th}_k = e^{-k\beta\omega_0}/\sum_{k=0}^N e^{-\beta k\omega_0}$ is the thermal occupation probability of the kth energy eigenstate. Here, we consider the following master equation

$$\partial_t\rho = -i[H,\rho] + \gamma_\downarrow \mathcal{D}[L_{\omega_0}]\rho + \gamma_\uparrow \mathcal{D}[L^\dagger_{\omega_0}]\rho, \tag{C1}$$

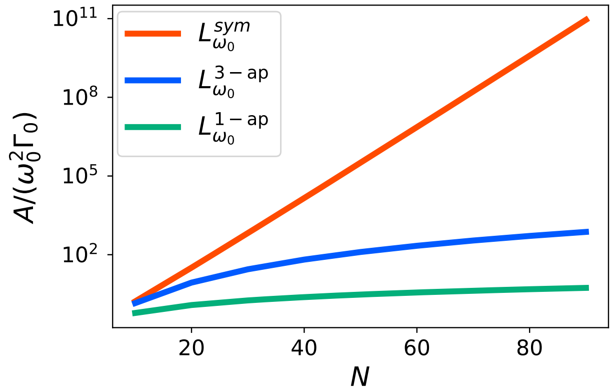

FIG. 4. Scaling of A for different jump operators when the density matrix is given by $\rho^{\rm sym}_{\rm th}$. The green, blue, and red curves are calculated by using $L^{\rm 1\text{-}ap}_{\pm\omega_0}$, $L^{\rm 3\text{-}ap}_{\pm\omega_0}$, and $L^{\rm sym}_{\pm\omega_0}$, respectively. See also the Supplemental Material [41] for further details of the scaling of A. The parameters are $\omega_0 = 0.7$, $\beta = 5$.

where $L_{\omega_0} = \{L^{\rm 1\text{-}ap}_{\omega_0}, L^{\rm 3\text{-}ap}_{\omega_0}, L^{\rm sym}_{\omega_0}\}$, $L^\dagger_{\omega_0} = L_{-\omega_0}$, $\gamma_\downarrow = \Gamma_0/(1+e^{-\beta\omega_0})$ and $\gamma_\uparrow = \Gamma_0/(1+e^{\beta\omega_0})$ satisfy the detailed balance condition $\gamma_\downarrow/\gamma_\uparrow = e^{\beta\omega_0}$. Note that $\rho^{\rm sym}_{\rm th}$ is the steady state of Eq. (C1) when the initial state is prepared in the symmetric Dicke subspace [e.g., $\rho^{\rm sym}(0) = \sum_k p_k(0)\rho^{\rm sym}_k$], because $L^{\rm 1\text{-}ap}_{\pm\omega_0}$, $L^{\rm 3\text{-}ap}_{\pm\omega_0}$, and $L^{\rm sym}_{\pm\omega_0}$ satisfy the strong symmetry condition. In Fig. 4, we plot $A = \sum_{\omega=\pm\omega_0}\omega^2 A_\omega(\rho^{\rm sym}_{\rm th}, L_\omega)$, where its analytical expression, including the scaling of $A = O(N)$ for $L^{\rm 1\text{-}ap}_{\pm\omega_0}$ and $A = O(N^3)$ for $L^{\rm 3\text{-}ap}_{\pm\omega_0}$ is obtained in the Supplemental Material [41]. From Fig. 4, we also find that A scales exponentially for $L^{\rm sym}_{\pm\omega_0}$.